Superalloys 2012: 12th International Symposium on Superalloys
Edited by: Eric S. Huron, Roger C. Reed, Mark C. Hardy, Michael J. Mills, Rick E. Montero, Pedro D. Portella, Jack Telesman
TMS (The Minerals, Metals & Materials Society), 2012

ALLOYING EFFECTS IN THE γ' PHASE OF CO-BASED SUPERALLOYS

Alessandro Mottura[1], Anderson Janotti[1], Tresa M. Pollock[1]

[1]Materials Department, University of California - Santa Barbara, Santa Barbara CA 93106-5050

Keywords: Co-based Superalloys, *Ab initio* Modeling, Stacking Fault Energy

Abstract

New γ/γ' Co-based alloys appear to be a promising set of materials for use in the hottest parts of gas turbines. Recent work has shown that these alloys behave similar to conventional Ni-based superalloys and preliminary designs have produced alloys with remarkable strength at high temperatures. Understanding the behavior of solute elements in these alloys is essential for improving their properties and designing viable alloys. In this work, *ab initio* simulations are used to study the effects of additional elements on fault energies in the γ' phase. Initial investigation shows that both Ta and Ti retain a strong preference for the second sub-lattice in the γ' phase. Calculations also show that these elements increase the superlattice intrinsic stacking fault energy of the γ' precipitates while promoting the stability of the γ' phase relative to other crystal structures. This work indicates that the stability and resistance to dislocation penetration of the γ' phase in these alloys are closely linked and are strongly affected by chemical bonding rather than the size of solute atoms.

Introduction

The recent development of new Co-based superalloys is based on the discovery of the γ' phase in the Co-Al-W ternary phase diagram [1] and the presence of a $\gamma+\gamma'$ phase field in the Co-rich corner of the ternary diagram (see Figure 1). Similar to Ni-based superalloys, the γ' phase in Co-based superalloys possesses a $L1_2$ crystal structure, with roughly equal fractions of Al and W randomly distributed on the second sublattice (see Figure 1). The γ' phase does not appear in either the Co-Al or the Co-W binary phase diagrams at typical service temperatures: γ-Co (*fcc*) and β-CoAl (B_2) coexist in the Co-Al binary phase diagram, while a Co_3W intermetallic with the $D0_{19}$ crystal structure is the most stable phase in the Co-W binary phase diagram. The lattice mismatch between the γ and γ' phase in the ternary system is 0.53 %, which is small enough to allow the γ' precipitates to grow coherently within the γ matrix, maintaining a cuboidal morphology [1, 2].

Initial attempts to produce 4- and 5-element γ'-strengthened superalloys based on the Co-Al-W ternary system resulted in alloys with extraordinary yield strengths at high temperature [2], high melting temperature [3] and low segregation during solidification [4]. Additionally, it has been observed that the addition of 2 at.% Ta to a single-crystal Co-Al-W ternary alloy results in a flow stress above 500 MPa at 1243 K [2]. Higher densities of super-lattice intrinsic stacking faults (SISFs) were observed within the γ' precipitates in deformed samples of the Ta containing alloy when compared to a simple ternary alloy. These stacking faults arise from the combination of two full $a/2\langle 101\rangle$ dislocations in the γ phase forming an $a/3\langle 112\rangle$ that shears the γ' precipitates, creating a SISF, and an $a/6\langle 112\rangle$ which remains at the γ/γ' interface (see Figure 2). This observation led to the hypothesis that Ta may have an effect on SISF energy (ΔE_{SISF}) [2].

Further improvements in the properties of these materials will require higher order alloying additions that raise the γ' solvus temperature and improve creep properties of these materials [3]. It follows that understanding effects of solute elements in the γ and γ' phase on the properties of Co-based superalloys is essential for the development of these alloys. *Ab initio* simulations can be instrumental in providing insight that will accelerate the design of these alloys. In this research, *ab initio* methods have been employed to investigate the effects of Ta and Ti, but other elements have been studied to establish trends across the periodic table.

Theory

Special Quasi-random Structures (SQSs)

Simulating a random arrangement of solute atoms *ab initio* is not trivial since periodic boundary conditions enforce periodicity of the lattice. The underlying concept to Special Quasi-random Structures (SQSs) is to pick configurations of a small number of

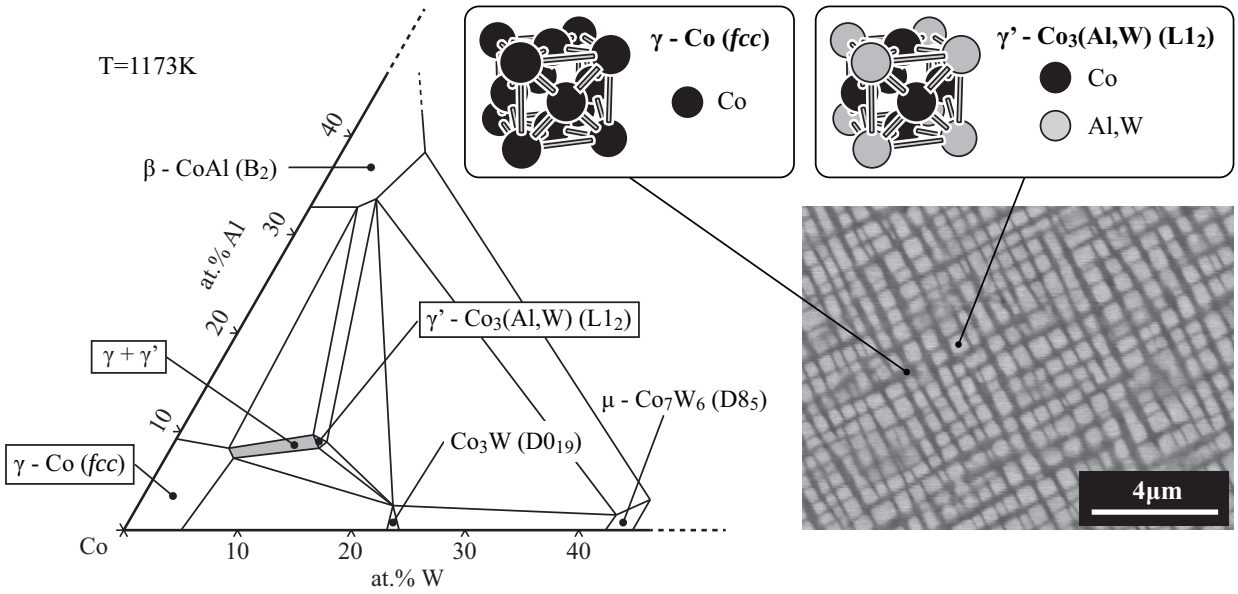

Figure 1: A schematic of the Co-Al-W ternary phase diagram at 1173 K with a representation of the unit cells for the γ and γ' phase in the Co-Al-W system. The SEM micrograph (courtesy of M. Titus) shows the typical microstructure that can be obtained from compositions within the $\gamma+\gamma'$ phase field.

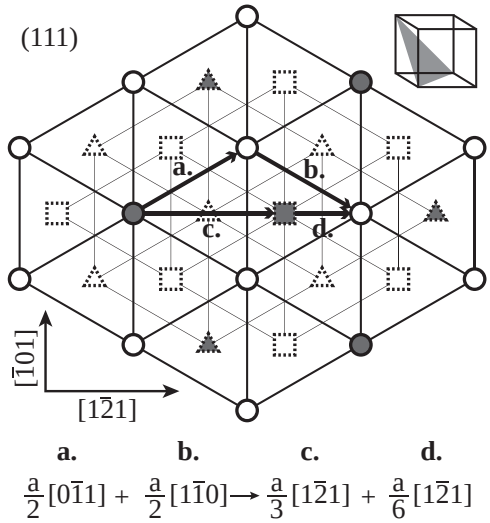

Figure 2: A schematic of the observed dislocation reaction.

A and B atoms on a given lattice, $\boldsymbol{\sigma}$, which replicate a random distribution of the atoms in an infinite cell [5]. This is achieved by calculating the correlation functions, $\overline{\Pi}_{k,m}(\boldsymbol{\sigma})$, for the most important atomic figures (*e.g.* 1st neighbor pairs, 2nd neighbor pairs, 1st neighbor triplets, *etc.*). The figures are defined by k, the number of vertices in a figure, and m, the distance between the vertices in that figure. Therefore, $\overline{\Pi}_{k,m}(\boldsymbol{\sigma})$ for each figure can be calculated using Equation 1.

$$\overline{\Pi}_{k,m}(\boldsymbol{\sigma}) = \frac{1}{N_{k,m}} \sum_{n}^{N_{k,m}} \prod_{i}^{k} \sigma_i \qquad (1)$$

In Equation 1, $N_{k,m}$ is the total number of k, m figures in a given configuration and σ_i are the spin variables that describe whether a lattice site is occupied by a A atom ($\sigma_i = +1$) or a B atom ($\sigma_i = -1$). For a random distribution of an equal concentration of A and B atoms on a lattice, $\overline{\Pi}_{k,m}(\boldsymbol{\sigma}_{\text{random}}) = 0$ for all figures in the configuration. Therefore, many different configurations can be compared to an ideal random arrangement of A and B atoms and those configurations with similar $\overline{\Pi}_{k,m}(\boldsymbol{\sigma})$ can be selected.

Jiang used this approach to investigate the stability of $L1_2$-$Co_3(Al,W)$ [6]. Additionally, SQSs have been

used extensively in conjunction with the ANNNI model to efficiently calculate the effect of relatively high concentrations of solute elements on the ΔE_{ISF} of Fe [7, 8, 9].

Axial Next Nearest Neighbour Ising model (ANNNI)

Unfortunately, SQSs cannot be used to calculate ΔE_{SISF} with the traditional supercell approach. This approach would involve building a supercell large enough to contain two or three SISF stacked at a sufficient distance that interactions between the faults are kept at a minimum. This usually leads to cells elongated in the direction normal to the faults which, in this case, would also need to be larger in the directions in-plane with the fault in order to reproduce a random arrangement of Al and W atoms on the second sub-lattice. A solution to this problem is provided by the axial next nearest neighbor (ANNNI) model [10].

Within the ANNNI model the total energy of a system made of equivalent planes stacked in particular order can be described with an Ising model, as shown in Equation 2.

$$E_{\mathrm{tot}} = J_0 - \sum_{m}^{M} J_m \sum_{n}^{N} \sigma_n \sigma_{n+m} \tag{2}$$

In Equation 2, n is an index defining each plane within the system made of N equivalent planes, σ_n is a spin variable that takes value $+1$ or -1 depending on whether the plane $n+1$ is correctly stacked with respect to plane n and J_m are expansion coefficients. The model can be expanded to include M^{th}-neighbor interactions, as shown in Equation 3.

$$E_{\mathrm{tot}} = J_0 - J_1 \sum_{n}^{N} \sigma_n \sigma_{n+1} - J_2 \sum_{n}^{N} \sigma_n \sigma_{n+2} - \dots \tag{3}$$

Consequently, the total energy of any arrangement of N close-packed $\{111\}$ planes, such as *fcc* $(ABCABC\dots)$, *hcp* $(ABAB\dots)$ and *fcc* containing an intrinsic stacking fault $(ABCBC\{ABC\}\dots)$ can be described in terms of the J_m expansion coefficients, as seen in Equation 4, 5 and 6 respectively.

$$E_{\mathrm{tot}}^{fcc}(N) = J_0 - NJ_1 - NJ_2 - NJ_3 - NJ_4 - \dots \tag{4}$$

$$E_{\mathrm{tot}}^{hcp}(N) = J_0 + NJ_1 - NJ_2 + NJ_3 - NJ_4 + \dots \tag{5}$$

$$E_{\mathrm{tot}}^{isf}(N) = J_0 + (4-N)\cdot J_1 + (4-N)\cdot J_2 + \dots \tag{6}$$

The energy of an intrinsic stacking fault, ΔE_{ISF}, is proportional to the difference between the total energies of a perfect (E_{tot}^{fcc}) and a faulted (E_{tot}^{isf}) systems composed of N $\{111\}$ planes. As a result, ΔE_{ISF} can also be described in terms of the J_m expansion coefficients and the area of the fault, A, as shown in Equation 7.

$$\Delta E_{\mathrm{ISF}} = \frac{E_{\mathrm{tot}}^{isf}(N) - E_{\mathrm{tot}}^{fcc}(N)}{A} = \frac{\sum_{m=1}^{M} 4J_m}{A} \tag{7}$$

Therefore, ΔE_{ISF} can be re-written in terms of the total energy of small periodical arrangements of $\{111\}$ planes. For example, discarding elements beyond J_1 yields Equation 8.

$$\Delta E_{\mathrm{ISF}} = \frac{2\left(E_{\mathrm{tot}}^{hcp} - E_{\mathrm{tot}}^{fcc}\right)}{A} \tag{8}$$

Truncation depends on how many neighboring planes are needed in order to accurately describe ΔE_{ISF}. For metals, interactions are very short-range and $J_1 >> J_2, J_3, J_4$. Also, it should be noted that discarding all elements beyond J_1 renders ΔE_{ISF} and the extrinsic stacking fault energy, ΔE_{ESF}, equivalent. Thus, discarding all elements beyond J_1 is sufficient for most metals since the difference between ΔE_{ISF} and ΔE_{ESF} is small relative to other fault energies [10, 11, 12]. The observation that the ΔE_{ISF} is closely related to the difference between the formation energies of the *fcc* and *hcp* phases has been well known and explained in the literature [13, 14, 12] and the ANNNI model has been used extensively to calculate the ΔE_{ISF} of several transition metals [15], as well as the effect of solute atoms on the ΔE_{ISF} of Fe [7, 8, 9] and Ni [16] and compared well with ΔE_{ISF} obtained using the conventional supercell approach. In the case of the $L1_2$ ordered compound, a SISF is effectively equivalent to the ISF for the super-lattice. Therefore, ΔE_{SISF} is linked to the difference in energy between the $L1_2$ and $D0_{19}$ crystal structures.

Methodology

Density functional theory (DFT) calculations were performed using the Vienna *Ab initio* Simulation Package (VASP) [17, 18]. The Projector Augmented Wave (PAW) method [19, 20] was used to describe the electron-ion interactions. The spin-polarized Generalized Gradient Approximation (GGA) parameterized by Perdew, Burke and Ernzerhof [21] was used as an approximation of the exchange-correlation functional. Plane waves were included up to 300 eV, which was deemed sufficient for accurate convergence. For large super cells, the projector operators were evaluated in real space. The Monkhorst-Pack scheme was used to define the k-points and high accuracy was ensured by running calculations with a k-point density higher than $5 \cdot 10^5$ k-points/Å^{-3}. The electronic self-consistent loops were considered converged after the change in total energy between subsequent steps fell below 10^{-5} eV. Structure relaxations were stopped once the forces acting on all the ions fell below 10^{-3} eV/Å. Two 32-atom SQSs for each crystal structure ($L1_2$ and $D0_{19}$) were obtained using ATAT [22, 23, 24, 25], matching the correlation functions of an ideal random distribution of Al and W atoms up to 4$^{\text{th}}$ neighboring 2$^{\text{nd}}$ sub-lattice atoms.

Results

The average formation energies of the SQSs of Co_3(Al,W) (relative to *hcp*-Co, *fcc*-Al and *bcc*-W) were -0.126 eV/atom and -0.110 eV/atom for the $L1_2$ and $D0_{19}$ crystal structure respectively. These results are in good agreement with previous work by Jiang [6]. At 0 K, although the $L1_2$ has a lower formation energy than $D0_{19}$, both structures are still ~ 0.06 eV above the lowest energy configuration (α-Co + β-CoAl + $D0_{19}$-Co_3W). However, configurational and vibrational entropy may help stabilizing the $L1_2$ phase at higher temperatures.

Stacking fault energy

The ΔE_{SISF} of $L1_2$-Co_3(Al,W) is calculated from the total energies of the SQSs obtained from ATAT using Equation 8. In agreement with the literature, the total energies of the $D0_{19}$ SQSs were calculated at a volume equivalent to the ground state volume of the $L1_2$ SQSs [8]. This means that four distinct values of ΔE_{SISF} can be obtained from these four SQSs, since the energies of each of the $D0_{19}$ SQSs can be evaluated after making their volume equivalent to either of the $L1_2$ SQSs. All permutations lead to a ΔE_{SISF} in the range 89-93 mJ/m^2. These values can be compared to the γ' phase in Ni-based superalloys. A survey of the literature reveals values of ΔE_{SISF} for Ni_3Al ranging 40-147 mJ/m^2 as calculated with a variety of methods based on *ab initio* simulations [26, 27, 28, 29]. The large scatter in the literature is attributed to differences in the methodologies used to obtain these results. Using the ANNNI model, the ΔE_{SISF} of Ni_3Al was found to be 53 mJ/m^2. Calculating the ΔE_{SISF} of Ni_3Al via the same method serves two purposes. First, it can be observed that the value of ΔE_{SISF} obtained falls within the range of values obtained from previous studies, confirming that the ANNNI model can be used to predict ΔE_{SISF}. Second, the value of ΔE_{SISF} for Ni_3Al obtained with the ANNNI model can be directly compared to the value of ΔE_{SISF} for Co_3(Al,W). It can be observed that the ΔE_{SISF} of the γ' phase of Co-based superalloys is $\sim 75\,\%$ higher than the γ' of Ni-based superalloys.

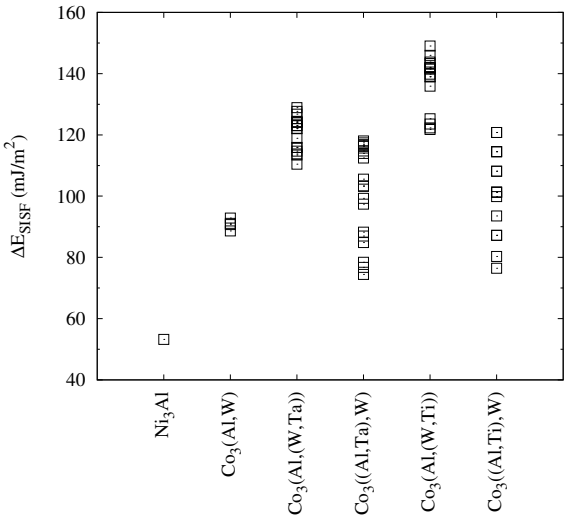

Figure 3: The superlattice intrinsic stacking fault energy (ΔE_{SISF}) of Ni_3Al, Co_3(Al,W) and Co_3(Al,W) with small additions of Ta and Ti.

Solute effects on stacking fault energy

In order to study the effect of solute atoms on the ΔE_{SISF} of $L1_2$-Co_3(Al,W), the generation of a separate set of SQSs with varying amounts of Al, W

and additional solute atoms (X) on the second sub-lattice would be desirable. However, obtaining these structures with $\overline{\Pi}_{k,m}$ comparable to those of an ideal random arrangement of Al, W and X atoms is impractical due to computational constraints. Even if these SQSs were available, they would need to be very large in order to accommodate dilute solute atoms (< 5 at.%). As a result, simulating these SQSs *ab initio* would also be computationally prohibitive.

Instead, as a first step, we aim to study the effects of Ta and Ti on the total energies of the same set of 32-atom SQSs used above. In the 32-atom supercells, the substitution of an Al or W atom with a solute atom would lead to a solute concentration of ~ 3 at.%. The substitution with a solute atom raises two concerns. First, each of the 8 sites of the second sub-lattice is inequivalent. This is because, although each site is surrounded by 12 Co nearest neighbors, higher order neighbors are different at each site. Therefore, we expect small differences in total energy when the substitutional atom is located at different sub-lattice sites within supercells of equal composition. Second, the substitution with a solute atom will lead to different concentrations of Al and W, yielding 32-atom supercells with formula $Co_{24}Al_3W_4X_1$ or $Co_{24}Al_4W_3X_1$. Therefore, the effect of solute atoms on the ΔE_{SISF} of the γ' phase may differ depending on whether a particular solute atom is substituting an Al or a W atom. As a result, this study is expected to yield the effect of Ta and Ti on ΔE_{SISF} when used as a substitute for either Al or W.

From these values, the impurity formation energy (E_{IF}) of a Ta and Ti substitution (replacing either an Al, a W or a Co atom) can be obtained using the same method adopted by Chen and Wang [30, 31]. Chen and Wang calculated E_{IF} using Equation 9 [30, 31].

$$E_{\mathrm{IF}} = E_b^{\mathrm{def.}} - E_b^{\mathrm{pure}} \tag{9}$$

In Equation 9, E_b^{pure} and $E_b^{\mathrm{def.}}$ are the binding energies of the perfect and faulted structure, calculated using Equation 10 [30, 31].

$$E_b = E_{\mathrm{tot}} - \sum_i n_i E_i \tag{10}$$

In Equation 10, E_{tot} is the total energy of a given structure, n_i is the number of i atoms in the structure and E_i is the energy of the atoms in their reference state [30]. It should be pointed out that the E_{IF} calculated using this method is not the defect formation energy, and the supercells used to obtain the necessary binding energies (E_b^{pure} and $E_b^{\mathrm{def.}}$) have slightly different compositions. Nevertheless, the E_{IF} can provide some insight into the relative site preference of Ta and Ti in Co_3(Al,W). It can be seen that placing a Ta or a Ti atom at the Al/W sites yields negative E_{IF}, suggesting the presence of an energy advantage in creating the defect (see Table 1). Conversely, placing a Ta atom in the Co sites yields a slightly positive E_{IF} (see Table 1). Placing a Ti atom at the Co sites leads to a negative, albeit small, E_{IF} (see Table 1). This confirms that both Ta and Ti would be expected to preferentially sit on the second sub-lattice (Al/W). Although the results of this study quantitatively differ from those obtained by Chen and Wang [30], relationships between the different E_{IF} are equivalent, with both studies indicating that Ta and Ti would sit on the second sub-lattice. Differences in absolute values are most likely due to the fact that Chen and Wang used an ordered supercell of $L1_2$-Co_3(Al,W), whereas this study adopts SQSs to simulate the random distribution of Al and W on the second sub-lattice. This is particularly apparent when the solute atoms are used to substitute a Co atom: the ordered $L1_2$-Co_3(Al,W) supercells contain three inequivalent Co sites, whereas in the SQSs adopted in this study virtually every Co site is inequivalent. Therefore, the distribution of atoms surrounding these point defects is different in the two studies.

Table 1: The impurity formation energy of a Ta and Ti substitution within the different sites in the SQSs compared to those calculated by Chen and Wang [30, 31].

	Current Work	Ref. [30, 31]
$E_{\mathrm{IF}}^{\mathrm{Ta:Al}}$ (eV)	-0.365	-0.241
$E_{\mathrm{IF}}^{\mathrm{Ta:W}}$ (eV)	-0.423	-0.517
$E_{\mathrm{IF}}^{\mathrm{Ta:Co}}$ (eV)	0.113	(-0.205)
$E_{\mathrm{IF}}^{\mathrm{Ti:Al}}$ (eV)	-0.361	-0.393
$E_{\mathrm{IF}}^{\mathrm{Ti:W}}$ (eV)	-0.349	-0.697
$E_{\mathrm{IF}}^{\mathrm{Ti:Co}}$ (eV)	-0.076	(-0.059)

Similar to the $L1_2$ SQSs, Ta and Ti atoms can also substitute Al ad W sites in the $D0_{19}$ SQSs. As a result, also in this case 8 supercells can be obtained for $D0_{19}$-$Co_{24}Al_3W_4Ta_1$, $D0_{19}$-$Co_{24}Al_4W_3Ta_1$, $D0_{19}$-$Co_{24}Al_3W_4Ti_1$ and $D0_{19}$-$Co_{24}Al_4W_3Ti_1$. Using

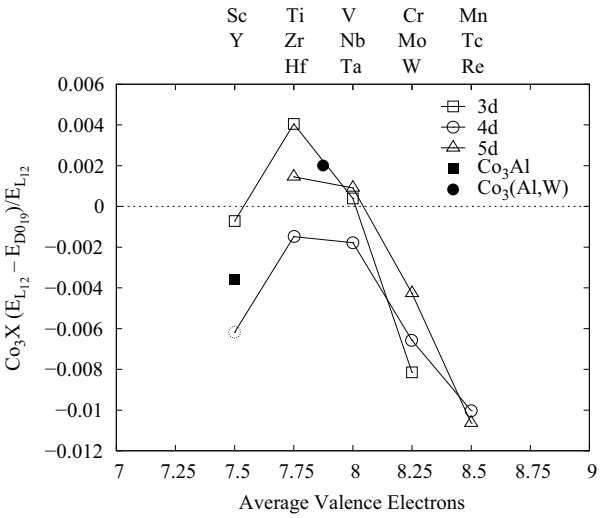

Figure 4: The relative energies of $L1_2$-Co_3X and $D0_{19}$-Co_3X, where X is Sc, Ti, V, Cr, Y, Zr, Nb, Mo, Tc, Hf, Ta, W and Re, plot against the average number of valence electrons per atom

the total energies of the fully relaxed $L1_2$ supercells and the total energies of the $D0_{19}$ supercells, obtained at volumes equivalent to the volumes of the $L1_2$ supercells, several distinct values of ΔE_{SISF} can be obtained for $L1_2$-Co_3((Al,Ta),W), $L1_2$-Co_3(Al,(W,Ta)), $L1_2$-Co_3((Al,Ti),W) and $L1_2$-Co_3(Al,(W,Ti)). The results, along with the ΔE_{SISF} for Ni_3Al and Co_3(Al,W) are shown in Figure 3. These calculations show that both Ta and Ti additions are expected to raise the ΔE_{SISF} of the γ' phase of Co-based superalloys, by stabilizing the $L1_2$ crystal structure relative to the $D0_{19}$ crystal structure (see Equation 8).

Effect of chemistry on stacking fault energy

The effect of solute atoms and, more generally, composition on ΔE_{SISF} can be explained by considering d-band effects. It has been shown that relative energy differences between different crystal structures (*i.e. fcc* and *hcp*) are strongly linked to the average number of valence electrons in a given compound [32, 33]. These trends have been observed for *fcc*, *hcp*, *bcc* and *tcp* phases in 3d, 4d and 5d transition metals [32, 33]. In this case, it has been shown that ΔE_{SISF} is proportional to the difference in energy between the $L1_2$ and $D0_{19}$ crystal structures. Therefore, ΔE_{SISF} is also expected to follow a trend across the periodic table. In order to investigate this theory, the energies of $L1_2$-Co_3X and $D0_{19}$-Co_3X (where X=Sc, Ti, Vn, Cr, Y, Zr, Nb, Mo, Tc, Hf, Ta, W and Re) were computed using DFT. The results were then plotted against the average number of valence electrons per atom for each compound, as shown in Figure 4. It can be seen that the $D0_{19}$ crystal structure has a lower energy than the $L1_2$ crystal structure for both Co_3W and Co_3Al. However, the $L1_2$ crystal structure is expected to have a lower energy than the $D0_{19}$ crystal structure for compounds with average electron numbers 7.75-8 e^-/atom. The stoichiometric γ' phase of Co-based superalloys (Co_3(Al,W)) also appears to fall within this trend.

Discussion

A previous study has demonstrated a strong positive influence of Ta additions to γ'-strengthened Co-based superalloys on the high temperature yield strength [2]. The authors observed a high work hardening rate and an unusually high superlattice intrinsic stacking fault density after high temperature deformation at 1270 K in Ta-containing samples when compared to the simple ternary alloy [2]. The activation of the $a/3\langle 112\rangle\{111\}$ slip system in the γ' precipitates at higher temperatures, which results in the observed superlattice intrinsic stacking faults, is linked to the high-temperature strengths observed in single-crystal Ni- and Co-based superalloys [2]. The authors suggested that a higher density of SISFs in Ta-containing alloys could be caused by additions of Ta lowering the ΔE_{SISF} of the γ' phase in Co-based superalloys [2]. This study has employed first-principles calculations to examine this hypothesis.

According to the results shown in the previous section, Ta additions are expected to increase the ΔE_{SISF} of the γ' phase of Co-based superalloys, and it would then be expected that precipitate shearing by $a/3\langle 112\rangle$ superlattice partial dislocations would be influenced by Ta additions. This is a direct consequence of the fact that Ta additions lower the formation energy of the $L1_2$ phase relative to the $D0_{19}$ phase (see Equation 8). This may be expected since experimentally Ta is added to promote the formation and stability of the γ' precipitates and hinder the formation of detrimental phases such as Co_3W [1, 2].

Since Ta additions do not lower the ΔE_{SISF} of the γ' phase, the anomalous work hardening effect generated by Ta must not be directly due to the presence of SISFs observed within the γ' precipitates. A higher

ΔE_{SISF} would require a higher shear stress for initial penetration of dislocations into the Ta-containing $L1_2$ phase compared to the simple Co_3(Al,W) ternary γ' phase. Examination of the TEM micrographs in [2] reveals that the volume fraction of γ' phase is considerably higher in the Ta-containing alloy. Additionally, deformation tests were carried out at temperatures close to the γ' solvus (1300 K and 1350 K for the simple ternary and Ta-containing alloy respectively). As a result, the higher volume fraction of γ' precipitates associated with the higher stability of this phase, in conjunction with the higher shear stress required to initiate $a/3\langle 112\rangle\{111\}$ slip within the precipitates, is expected to generate the strengthening observed with the addition of Ta.

This work has also shown that Ti may also generate similar strengthening effects when compared to Ta. Indeed, according to DFT, small additions of Ti are expected to increase the ΔE_{SISF} even further than Ta. This, along with the fact that Ti is lighter than Ta and W, makes Ti extremely interesting in the development of new γ'-strengthened Co-based superalloys. Adding Ti may lower the density of these alloys while improving creep properties and promoting the formation of γ' at higher temperatures. Recent work by Titus *et al* [34] has shown that Ti additions to these alloys lead to improved creep properties.

The beneficial effect that Ta and Ti have on the ΔE_{SISF} of γ' can be strongly linked to d-band effects. If higher ΔE_{SISF} is required in order to inhibit γ' precipitates penetration at higher temperatures, then alloying with any of the elements from group 4 and 5 of the periodic table (Ti, V, Zr, Nb, Hf and Ta) may be desirable.

Conclusions

- The ΔE_{SISF} of the γ' phase of Co-based superalloys is $\sim 91\,\mathrm{mJ/m^2}$, approximately a factor of two higher than the ΔE_{SISF} of the γ' phase of Ni-based superalloys ($\sim 53\,\mathrm{mJ/m^2}$), as calculated with the same procedure.
- The addition of Ta and Ti increases the ΔE_{SISF} of the γ' phase of Co-based superalloys, since both elements lower the energy of the $L1_2$ crystal structure relative to the $D0_{19}$ crystal structure.
- The observed beneficial effect of Ta and the predicted beneficial effect of Ti can be explained by considering changes in average valence electron concentration resulting from these additions. This observation provides a clear pathway for the development of new γ'-strengthened Co-based superalloys.
- Increasing ΔE_{SISF}, these elements may improve the resistance of the precipitates to initial shearing by $a/3\langle 112\rangle$ partial dislocations, ultimately resulting in better high temperature properties. It should be pointed out that these elements, beside increasing ΔE_{SISF}, have been observed to raise the γ' solvus temperature, which is also desirable for high temperature mechanical properties.

Acknowledgements

The authors acknowledge funding from the NSF DMR Grant Number 1008659 and the computational facilities provided by Teragrid through account numbers TG-DMR110001 and TG-DMR070072N.

References

[1] J. Sato, T. Omori, K. Oikawa, I. Ohnuma, R. Kainuma, and K. Ishida. Cobalt-base high-temperature alloys. *Science*, 312(5770):90–91, 2006.

[2] A. Suzuki and T. M. Pollock. High-temperature strength and deformation of γ/γ' two-phase CoAlW-base alloys. *Acta Mater.*, 56(6):1288–1297, 2008.

[3] T. M. Pollock, J. Dibbern, M. Tsunekane, J. Zhu, and A. Suzuki. New Co-based γ/γ' high-temperature alloys. *JOM*, 62(1):58–63, 2010.

[4] M. Tsunekane, A. Suzuki, and T. M. Pollock. Single-crystal solidification of new Co-Al-W-base alloys. *Intermetallics*, 19:636–643, 2011.

[5] A. Zunger, S.-H. Wei, L. G. Ferreira, and J. E. Bernard. Special quasirandom structures. *Phys. Rev. Lett.*, 65(3):353–356, 1990.

[6] C. Jiang. First-principles study of Co_3(Al,W) alloys using special quasi-random structure. *Scr. Mater.*, 59(10):1075–1078, 2008.

[7] L. Vitos, J.-O. Nilsson, and B. Johansson. Alloying effects on the stacking fault energy in austenitic stainless steels from first-principles theory. *Acta Mater.*, 54(14):3821–3826, 2006.

[8] A. Dick, T. Hickel, and J. Neugebauer. The effect of disorder on the concentration-dependence of stacking fault energies in $Fe_{1-x}Mn_x$ – a first principles study. *Mater. Technol.*, 80(9):603–608, 2009.

[9] A. Abbasi, A. Dick, T. Hickel, and J. Neugebauer. First-principles investigation of the effect of carbon on the stacking fault energy of Fe-C alloys. *Acta Mater.*, 59(8):3041–3048, 2011.

[10] P. J. H. Denteneer and W. van Haeringen. Stacking-fault energies in semiconductors from first-principles calculations. *J. Phys. C: Sol. St. Phys.*, 20(32):L883–L887, 1987.

[11] R. E. Voskoboinikov and C. M. F. Rae. A new γ-surface in $\{111\}$ plane in $L1_2$ Ni_3Al. *IOP Conference Series: Materials Science and Engineering*, 3:012009, 2009.

[12] J. P. Hirth and J. Lothe. *Theory of dislocations*. Krieger Publishing Company, Malabar, Florida, 1982.

[13] T. Ericsson. The temperature and concentration dependence of the stacking fault energy in the Co-Ni system. *Acta Metall.*, 14(7):853–865, 1966.

[14] K. Ishida. Direct estimation of stacking fault energies by thermodynamic analysis. *Phys. Status Solidi A*, 36(2):717–728, 1976.

[15] N. M. Rosengaard and H. L. Skriver. Calculated stacking-fault energies of elemental metals. *Phys. Rev. B*, 47(19):12865–12873, 1993.

[16] M. Chandran and S. K. Sondhi. First-principle calculation of stacking fault energies in ni and nico alloy. *J. Appl. Phys.*, 109(10):103525, 2011.

[17] G. Kresse and J. Furthmuller. Efficient iterative schemes for ab initio total-energy calculations using a plane-wave basis set. *Phys. Rev. B*, 54(16):11169–11186, 1996.

[18] J. Hafner. Materials simulations using VASP - a quantum perspective to materials science. *Comput. Phys. Commun.*, 177(1-2):6–13, 2007.

[19] P. E. Blöchl. Projector augmented-wave method. *Phys. Rev. B*, 50(24):17953–17979, 1994.

[20] G. Kresse and D. Joubert. From ultrasoft pseudopotentials to the projector augmented-wave method. *Phys. Rev. B*, 59(3):1758–1775, 1999.

[21] J. P. Perdew, K. Burke, and M. Ernzerhof. Generalized gradient approximation made simple. *Phys. Rev. Lett.*, 77(18):3865–3868, 1996.

[22] A. van de Walle, M. Asta, and G. Ceder. The alloy theoretic automated toolkit: A user guide. *CALPHAD*, 26(4):539–553, 2002.

[23] A. van de Walle and G. Ceder. Automating First-Principles Phase Diagram Calculations. *J. Phase Equilib.*, 23:348, 2002.

[24] A. van de Walle. Multicomponent multisublattice alloys, nonconfigurational entropy and other additions to the Alloy Theoretic Automated Toolkit. *CALPHAD*, 33(2):266–278, 2009.

[25] G. L. W. Hart and R. W. Forcade. Algorithm for generating derivative structures. *Phys. Rev. B*, 77(22):224115, 2008.

[26] C. L. Fu and M. H. Yoo. All-electron total-energy theory of crystal elasticity – $L1_2$-ordered alloys. *Philos. Mag. Lett.*, 58(4):199–204, 1988.

[27] N. M. Rosengaard and H. L. Skriver. Ab initio study of antiphase boundaries and stacking faults in $L1_2$ and DO_{22} compounds. *Phys. Rev. B*, 50(7):48484858, 1994.

[28] G. Schoeck, S. Kohlhammer, and M. Fahnle. Planar dissociations and recombination energy of [110] superdislocations in Ni_3Al: Generalized Peierls model in combination with ab initioelectron theory. *Philos. Mag. Lett.*, 79(11):849–857, 1999.

[29] O. N. Mryasov, Y. N. Gornostyrev, A. van Schilfgaarde, and A. J. Freeman. Superdislocation core structure in $L1_2$ Ni_3Al, Ni_3Ge and Fe_3Ge: Peierls-Nabarro analysis starting from ab-initio GSF energetics calculations. *Acta Mater.*, 50(18):4545–4554, 2002.

[30] M. Chen and C. Y. Wang. First-principles investigation of the site preference and alloying effect of Mo, Ta and platinum group metals in γ'-$Co_3(Al,W)$. *Scr. Mater.*, 60(8):659–662, 2009.

[31] M. Chen and C. Y. Wang. First-principle investigation of 3d transition metal elements in γ'-$Co_3(Al,W)$. *J. Appl. Phys.*, 107(9):093705, 2010.

[32] T. Hammerschmidt, B. Seiser, R. Drautz, and D. G. Pettifor. Modeling topologically close-packed phases in superalloys: valence-dependent bond-order potentials based on ab-initio calculations. In R. C. Reed, P. Caron, T. Gabb, E. Huron, and S. Woodard, editors, *Superalloys 2008*, pages 847–853, Seven Springs, PA, USA, 2008. The Minerals, Metals and Materials Society, Warrendale, PA, USA.

[33] B. Seiser, T. Hammerschmidt, A. N. Kolmogorov, R. Drautz, and D. G. Pettifor. Theory of structural trends within 4d and 5d transition metal topologically close-packed phases. *Phys. Rev. B*, 83(22):224116, 2011.

[34] M. S. Titus, A. Suzuki, and T. M. Pollock. High Temperature Creep of New $L1_2$-containing Cobalt-base Superalloys. In E. Huron, M. Hardy, M. Mills, R. Montero, P. Portella, J. Telesman, and R. C. Reed, editors, *Superalloys 2012*, Seven Springs, PA, USA, 2012. The Minerals, Metals and Materials Society, Warrendale, PA, USA.